

Control of Electroosmotic Flow by Polymer Coating: Effects of the Electrical Double Layer

R. Qiao*

Department of Mechanical Engineering, College of Engineering and Science, Clemson University, Clemson, South Carolina 29634

Received April 3, 2006. In Final Form: May 22, 2006

We report on the molecular dynamics simulations of electroosmotic flow control by polymer coating. We show that polymer coating modulates the flow by rendering drag to fluids and by changing the ion distribution and ion–surface interactions in the electrical double layer. Because of the latter two effects, the polymer coating can even enhance the flow under certain conditions. Identifying the effects of these processes is crucial for the rational design of polymer coating for electroosmotic flow control.

Electroosmotic flow is an important type of electrokinetic transport.¹ When an ionic solution is in contact with a charged surface, an electrical double layer (EDL) with a net charge develops near the surface. If an external electrical field is applied in the direction tangential to the surface, the fluid will be dragged by the moving ions in an EDL and an electroosmotic flow is generated. Since the driving force for the flow resides only in the thin EDL (typically a few angstroms to tens of nanometers in thickness), the velocity profile of an electroosmotic flow is flat in most parts of the channel unless the channel width is comparable to the thickness of EDL. As a result, electroosmotic flow has a very small dispersion, and its flowrate scales more favorably than the pressure driven flow commonly used at macroscales.² Because of this, electroosmotic flow has become a popular fluid transport mechanism in micro- and nanofluidic systems.³

Effective control of electroosmotic flow is crucial in micro- and nanofluidic systems. For example, in microfluidic devices for protein analysis, electroosmotic flow typically needs to be suppressed to ensure a high-efficiency separation,⁴ whereas in capillary electrochromatography, it needs to be enhanced to improve the throughput.⁵ Among the many strategies proposed to control the electroosmotic flow, polymer coating (either by physical adsorption or covalent bonding) gained significant attention because in addition to controlling the electroosmotic flow effectively it can also reduce the analyte adsorption on the channel surface effectively, which is important for biomolecule separation applications.^{6–12} Though a large amount of empirical knowledge has been accumulated on the performance of different

polymer coatings, a thorough understanding of its flow control mechanisms is still missing. Few theoretical studies have been reported so far. Harden et al. studied the effects of polyelectrolyte coating on electroosmotic flow.¹³ Their scaling study focused on the coupling between deformation of the adsorbed polymer and the electroosmotic flow. Most recently, Tessier and Slater reported the molecular dynamics (MD) simulation of the control of electroosmotic flow by polymer coating.^{14,15} By using a coarse-grained description of the polymer and solvent, they were able to study the effect of polymer chain length and coating density systematically. Their simulation results provide direct verification of the scaling models proposed by Harden et al. These studies significantly advanced our understanding of the fundamental mechanisms of electroosmotic flow control by polymer coating. However, they focused mostly on the hydrodynamic aspect (e.g., drag of polymer on the fluid and deformation of polymer induced by the flow) of the flow control and did not address the physiochemical aspects of the flow control in details. In particular, the physical processes inside the EDL are usually modeled in a simplistic way. For example, theoretical analysis was typically performed at the thin EDL limit,¹³ and the rich physics within the EDL is lumped into an effective slip boundary condition at the channel surface. In the coarse-grained MD simulations,¹⁵ the chemical details of water and polymer (e.g., varying dielectric constant and the hydrophobicity of polymer chains) were not modeled, and thus the EDL is not modeled in details. As EDL plays a central role in determining the electroosmotic flow and effect of polymer coating on electroosmotic flow is known to correlate strongly with the physiochemical properties of solvent, polymer, and surfaces,⁸ it is important to complement the existing research by studying how the EDL is affected by the physiochemical properties of solvent and polymers and how this further affects the electroosmotic flow. Such a study, together with the prior studies, will further improve our understanding of the flow control mechanism and can help to develop reliable methods for designing and optimizing polymer coating for controlling electroosmotic flow.

Here we perform MD simulations to investigate how the electroosmotic flow is affected by the polymer coating at different grafting densities. Figure 1 shows a schematic of the simulation system. The system consists of a solid wall grafted with polymers

* To whom correspondence should be addressed. E-mail: rqiao@clemson.edu. URL: <http://www.clemson.edu/~rqiao>.

(1) Lyklema, J. *Fundamentals of interface and colloid science*; Academic Press: San Diego, CA, 1995.

(2) Probstein, R. F. *Physicochemical Hydrodynamics*; John Wiley & Sons: New York, 1994.

(3) Vilkner, T.; Janasek, D.; Manz, A. *Anal. Chem.* **2004**, *76*, 3373.

(4) Horvath, J.; Dolnik, V. *Electrophoresis* **2001**, *22*, 644.

(5) Wen, E.; Rathore, A. S.; Horvath, C. *Electrophoresis* **2001**, *22*, 3720.

(6) Hjerten, S. J. *Chromatogr.* **1985**, *347*, 191.

(7) Gao, Q. F.; Yeung, E. S. *Anal. Chem.* **1998**, *70*, 1382.

(8) Doherty, E. A. S.; Berglund, K. D.; Buchholz, B. A.; Kourkine, I. V.; Przybycien, T. M.; Tilton, R. D.; Barron, A. E. *Electrophoresis* **2002**, *23*, 2766.

(9) Cretich, M.; Chiari, M.; Pirri, G.; Crippa, A. *Electrophoresis* **2005**, *26*, 1913.

(10) Catai, J. R.; Tervahauta, H. A.; de Jong, G. J.; Somsen, G. W. J. *Chromatogr. A* **2005**, *1083*, 185.

(11) Bruin, G. J. M.; Chang, J. P.; Kuhlman, R. H.; Zegers, K.; Kraak, J. C.; Poppe, H. J. *Chromatography* **1989**, *471*, 429.

(12) Belder, D.; Warnke, J. *Langmuir* **2001**, *17*, 4962.

(13) Harden, J. L.; Long, D.; Ajdari, A. *Langmuir* **2001**, *17*, 705.

(14) Tessier, F.; Slater, G. W. *Macromolecules* **2005**, *38*, 6752.

(15) Tessier, F.; Slater, G. W. *Macromolecules* **2006**, *39*, 1250.

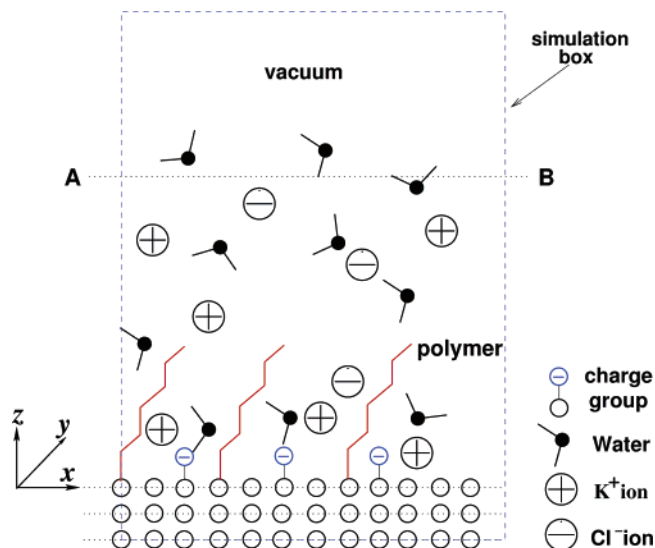


Figure 1. Schematic of the system under investigation. The system consists of a solid wall grafted with polymer and a slab of KCl solution covering the wall. The graft density is defined as the ratio between the number of polymer grafted on the surface and the number of atoms on the solid surface.

and a slab of KCl electrolyte covering the wall. The wall has a lateral dimension of $4.29 \times 4.29 \text{ nm}^2$, and a surface number density of $7.82/\text{nm}^2$. It consists of three layers of atoms arranged in a square lattice, and each atom is tethered to its lattice site by a spring. Sixteen charge groups, each consisting of a neutral silicon atom and an oxygen atom with $-e$ charge, are anchored to the top wall layer to produce a surface charge density (σ_s) of -0.14 C/m^2 . Ions are prevented from approaching the water–vacuum interface by an imaginary surface A–B, which reflects back the ions crossing the surface. The bulk concentration of the KCl solution is $0.95 \pm 0.05 \text{ M}$, and the thickness of the KCl solution layer is chosen such that the concentration of K^+ and Cl^- ions near surface A–B are the same. The bulk electrolyte concentration used here is higher than that typically used in microfluidic systems. This is caused by the limited length scale an MD simulation can explore. In MD simulation of electrokinetic transport, the system size must be several times larger than the Debye length. Using a low bulk concentration necessitates a large simulation system. For example, for a bulk concentration of 0.001 M (Debye length $\approx 10 \text{ nm}$), the characteristic length of the system must be at least tens of nanometers, which is beyond the computational power available at present. However, as the counterion concentration near the charged surface, the focus of the present study, is insensitive to the bulk concentration,¹⁶ the conclusions obtained here are applicable to the low bulk concentration scenarios. A strong external electric field of 0.24 V/nm is applied along the solid wall to induce an electroosmotic flow that can be retrieved from MD simulations. In such a set up, the region below surface A–B mimics the electroosmotic flow in a wide microchannel as the EDL (and thus the driving force for flow) exists only near the polymer-grafted wall. Such an electric field is several orders of magnitude higher than typically used in experiments. However, as the system is still in the linear response regime for the field strength considered here,¹⁷ the results obtained here should be applicable to laboratory situations.

Table 1. Summary of the Simulations Performed

case no.	polymer type	no. of polymer chains (grafting density)	surface A–B position	simulation box height
1		0 (0%)	$z = 2.8 \text{ nm}$	10.2 nm
2	$(\text{CH}_2)_{17}\text{COOH}$	16 (11%)	$z = 4.0 \text{ nm}$	14.4 nm
3	$(\text{CH}_2)_{17}\text{COOH}$	48 (33%)	$z = 4.0 \text{ nm}$	14.4 nm

Table 1 summarizes the three simulations performed. The electroosmotic flows were investigated at three polymer grafting densities (0%, 11%, and 33%). The polymer is chosen as $(\text{CH}_2)_{17}\text{COOH}$. It represents a broad class of amphiphilic polymers. In addition, it can be used to construct a dynamically responsive surface,^{18,19} which could be useful for modulating electroosmotic flow in the future. The hydrocarbon tail of the polymer is modeled by using the united atom approach, and the force field is taken from ref 20. To highlight their hydrophilic nature, the COOH headgroups are resolved in more detail by modeling each atom explicitly, and the OPLS all-atom force field was used.^{21,22} Water is modeled by using the SPC/E model²³ and the ions are modeled as charged Lennard-Jones atoms.²⁴ The wall atoms are modeled as Lennard-Jones spheres with force field parameters taken as that of the silicon atom in the Gromacs force field.^{25,26} Simulations were performed with a modified Gromacs 3.0.5.²⁶ Periodic boundary conditions are used in the x and y directions. A Nose thermostat²⁷ was used to maintain the fluid and wall temperature at 300 K . To avoid biasing the velocity profile, only the velocity component in the direction orthogonal to the flow was thermostated.²⁸ The electrostatic interactions were computed by using the PME slab method.²⁹ Other simulation details can be found in ref 17. Starting from a random configuration, each simulation system was simulated for 8 ns to reach a steady-state, followed by a 10 ns production run. The velocity and concentration profiles are obtained using the binning method.

Figure 2, panels a and b, shows the water density and ion concentrations near the bare solid surface. A significant layering of water that penetrates about 1 nm into the electrolyte solution is observed. Such a density oscillation is induced by the solid wall³⁰ and has been reported in many MD simulations of fluid–solid interfaces.¹⁷ The K^+ ion concentration reaches a peak ($c_{\text{K}^+} = 7.4 \text{ M}$) at $z = 0.53 \text{ nm}$, and the Cl^- ions are essentially depleted in the region $z < 0.55 \text{ nm}$. Both the K^+ and Cl^- ion concentrations approach the bulk electrolyte concentration ($c_{\text{KCl}} \approx 0.92 \text{ M}$) as moving away from the surface. For $z > 1.19 \text{ nm}$, the concentrations of both ions are essentially the same. The thickness of the EDL, as measured by the thickness of the region in which K^+ and Cl^- ion concentrations are different, is about 1.0 nm . In addition to these observations, which are in general agreement with the Poisson–Boltzmann theory¹ and coarse-grained atomistic

(18) Pei, Y.; Ma, J. *J. Am. Chem. Soc.* **2005**, *127*, 6802.

(19) Lahann, J.; Mitragotri, S.; Tran, T. N.; Kaido, H.; Sundaram, J.; Choi, I. S.; Hoffer, S.; Somorjai, G. A.; Langer, R. *Science* **2003**, *299*, 371.

(20) Shin, S.; Collazo, N.; Rice, S. A. *J. Chem. Phys.* **1992**, *96*, 1352.

(21) Jorgensen, W. L.; Maxwell, D. S.; Tirado-Rives, J. *J. Am. Chem. Soc.* **1996**, *118*, 11225.

(22) Jorgensen, W. L.; McDonald, N. A. *J. Phys. Chem. B* **1998**, *102*, 8049.

(23) Berendsen, H. J. C.; Grigera, J. R.; Straatsma, T. P. *J. Phys. Chem.* **1987**, *91*, 6269.

(24) Lee, S. H.; Rasaiah, J. C. *J. Phys. Chem.* **1996**, *100*, 1420.

(25) Berendsen, H. J. C.; van der Spoel, D.; van Drunen, R. *Comput. Phys. Commun.* **1995**, *91*, 43.

(26) Lindahl, E.; Hess, B.; van der Spoel, D. *J. Mol. Model.* **2001**, *7*, 306.

(27) Nose, S. *Mol. Phys.* **1984**, *52*, 255.

(28) Barrat, J. L.; Bocquet, L. *Phys. Rev. Lett.* **1999**, *82*, 4671.

(29) Yeh, I.; Berkowitz, M. *J. Chem. Phys.* **1999**, *111*, 3155.

(30) Karniadakis, G. E.; Beskok, A.; Aluru, N. R. *Microflows and nanoflows*; Springer: New York, 2005.

(16) Israelachvili, J. *Intermolecular and surface forces*; Academic Press: New York, 1992.

(17) Qiao, R.; Aluru, N. R. *J. Chem. Phys.* **2003**, *118*, 4692.

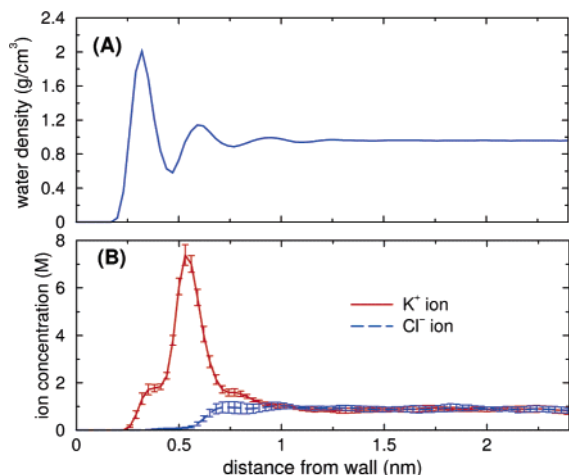


Figure 2. Density and concentration profiles for water (panel A) and K^+ and Cl^- ions (panel B) near the bare solid surface.

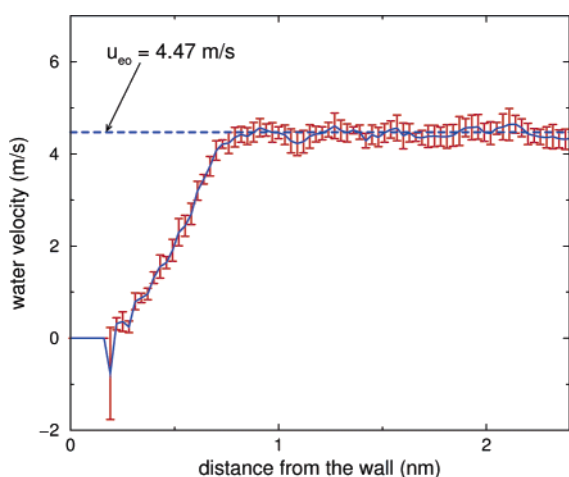


Figure 3. Electroosmotic velocity profile near the bare solid surface.

simulations,^{15,31,32} some fine features, such as the weak plateau of the K^+ ion concentration at $z = 0.75$ nm, are also observed. These features originate from the ion hydration effects near the surface^{17,33} and are difficult to obtain from coarse-grained simulations.

Figure 3 shows the water velocity profile near the channel surface. Consistent with the continuum models for electroosmotic flow, the water velocity profile is essentially flat outside the EDL. We compute the ζ potential of the bare solid surface by using

$$\zeta = -\frac{u_{eo}\eta}{\epsilon E_{ext}} \quad (1)$$

where u_{eo} is the water velocity outside the EDL and η and ϵ are the viscosity and permittivity of the solution, respectively. Using the viscosity and permittivity of the KCl solution,³³ the ζ potential of the solid surface is computed to be -19.5 ± 1.48 mV.

Figure 4a shows the water density profile near the solid surface grafted with 16 $(CH_2)_{17}COOH$ chains (grafting density, 11%). We observe that the significant layering of water observed near the bare wall is replaced by a gradual increase of water density as we move away from the surface, and the water density profile become bulklike for $z > 1.0$ nm. To understand this, we investigate

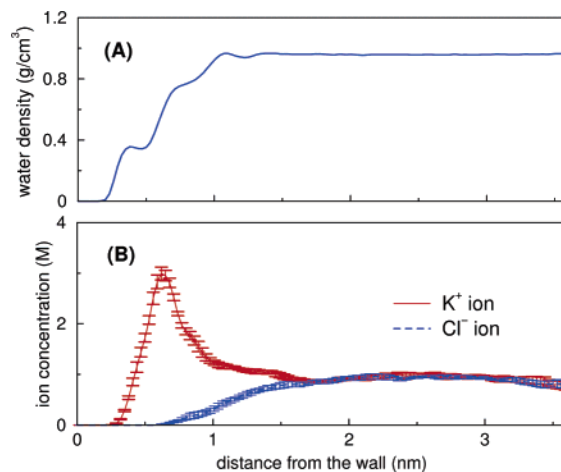


Figure 4. Density and concentration profiles for water (panel A) and K^+ and Cl^- ions (panel B) near the solid surface grafted with $(CH_2)_{17}COOH$ polymers (grafting density: 11%).

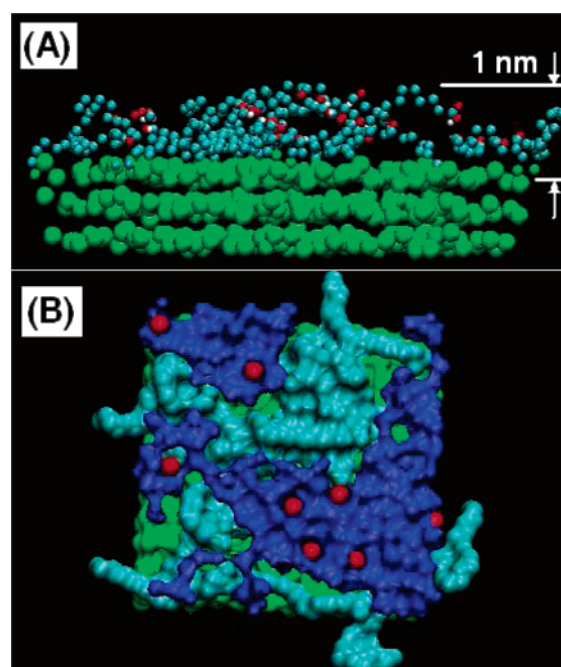


Figure 5. (A) Side view of the simulation system (grafting density: 11%). Only the polymer (cyan balls for the hydrocarbon tail, red and white balls for the COOH group) and solid surface (green balls) are shown for clarity. (B) Top view of the simulation system. Atoms are visualized as the volume they occupy, and only the molecules near the surface ($z < 0.8$ nm) is shown. The volume occupied by the polymer, water, K^+ ions are represented by cyan, blue and red colors, respectively. The probe radius of each atom is 1.4 Å. Images were rendered using VMD.^{34,35}

the polymer conformation near the surface. Figure 5a shows a snapshot of the polymers near the surface. We observe that most of the polymers are adsorbed on the surface in a “flat” conformation, and the polymers are confined to a region of 1.0 nm from the surface. Such a conformation is mainly caused by the strong hydrophobic interactions between the surface and the hydrophobic polymer chains. The absence of noticeable layering of water is not surprising as the density oscillation of fluid is known to decrease as the surface become less rigid; in the present case, the surface is now coated by a soft polymer layer.

Figure 4b shows the ion concentration near the surface. We observe that (1) compared to the bare surface case the first K^+ concentration peak ($z = 0.63$ nm) is significantly lower and is

(31) Thompson, A. P. *J. Chem. Phys.* **2003**, *119*, 7503.

(32) Cui, S. T.; Cochran, H. D. *Mol. Simulat.* **2004**, *30*, 259.

(33) Qiao, R.; Aluru, N. R. *Colloids Surf. A* **2005**, *267*, 103.

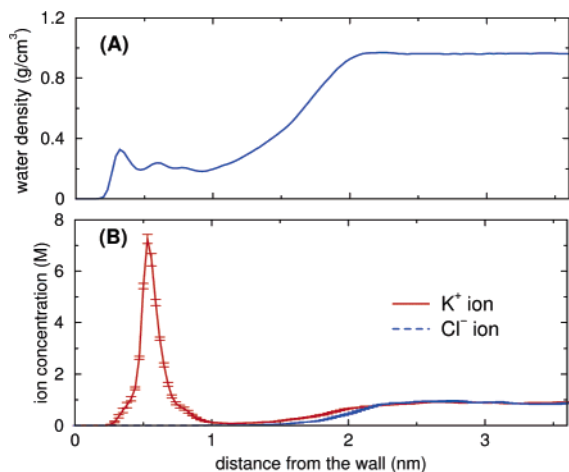


Figure 6. Density profiles for water (panel A) and K^+ and Cl^- ions (panel B) near the solid surface grafted with $(CH_2)_{17}COOH$ polymers (grafting density: 33%).

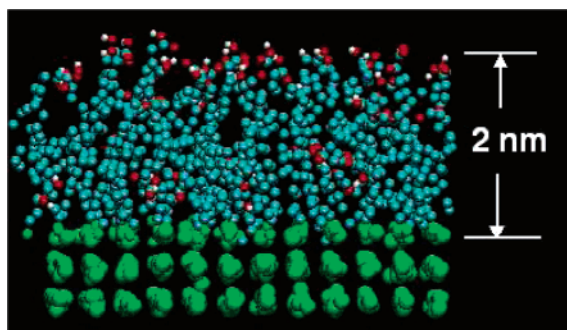


Figure 7. Side view of the simulation system (grafting density: 33%). Only the polymer (cyan balls for the hydrocarbon tail, red and white balls for the COOH group) and solid surface (green balls) are shown for clarity.

shifted about 0.1 nm away from the surface and (2) the EDL thickness is increased to about 1.8 nm, which is 80% wider compared to that in the bare surface case. Observation (1) is mainly caused by the unfavorable hydration of the K^+ ion near the surface. Figure 5b shows the volume that the molecules near the surface ($z < 0.8$ nm) occupy. We observe that a large fraction of the interfacial K^+ ions are located very close to the polymer and thus are not very well hydrated. In addition, the interfacial ions are not well hydrated by water molecules between the ion and the surface. This can be seen more clearly in Figure 4a: the water density for $z < 0.63$ nm is much lower compared to that for the bare surface case. Such unfavorable hydration makes it energetically costly for an ion to move toward the surface and thus lowers the ion concentration near the surface.³³ As the K^+ and Cl^- ion concentrations near the surface are lowered compared to the bare surface case, the EDL will extend further into the electrolyte solution. The electroosmotic velocity near the surface was also studied, and the ζ potential of the polymer-grafted surface is computed to be -27.0 ± 1.7 mV. Such an enhancement of electroosmotic flow is consistent with the general concepts that a more diffusive EDL will lead to a higher ζ potential.

Figure 6a shows the water density profile near the solid surface grafted with 48 $(CH_2)_{17}COOH$ chains (grafting density: 33%). Compared to the case of lower polymer-grafting density (see Figure 4), the water density is lower near the surface, and the water density deficiency extends deeper into the electrolyte. This can be understood by studying the polymer conformation shown in Figure 7. We observe that a significant amount of polymers are oriented toward the electrolyte. Adopting such a conformation

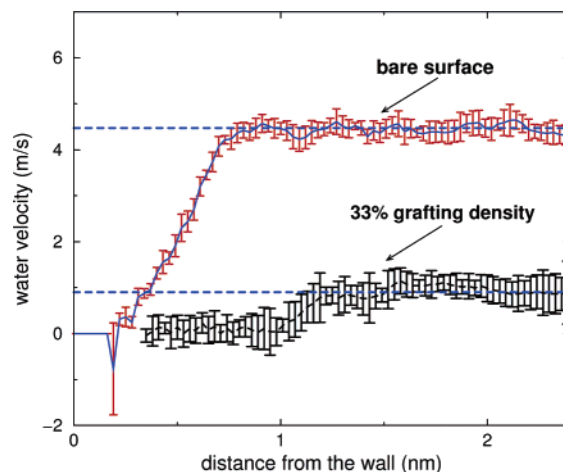


Figure 8. Comparison of the electroosmotic velocity profile near the solid surface for the bare surface and the surface grafted with $(CH_2)_{17}COOH$ polymers (grafting density: 33%). For the polymer-grafted surface case, the water velocity in region $0 < z < 0.3$ nm is not shown because of the large statistical error (caused by the low water density).

can reduce the steric hindrances between polymer chains, which becomes significant as the grafting density increases. Figure 6b shows the K^+ and Cl^- ion concentrations near the polymer-grafted surface. We observed that a significant amount of K^+ ions are adsorbed on the surface, whereas Cl^- ions are almost depleted in the region $z < 1.0$ nm. Such phenomena are most likely caused by the low dielectric constant in the interfacial region. Since the polymer has a much lower dielectric constant compared to water (e.g. solid organic polymers typically have dielectric constants between 4 and 5) and the water density is very low in the region $z < 1.0$ nm, the dielectric constant in this region will be much lower compared to that in the bulk. Because of the low dielectric constant in the interfacial region, the electrostatic interactions between the charged surface and the ions are little screened, and this leads to the significant adsorption of counterion and depletion of co-ion in the region.

Figure 8 shows the electroosmotic velocity profile near the surface, and the ζ -potential is found to be -3.93 ± 1.7 mV, i.e., the present polymer coating suppresses the electroosmotic flow near the original surface by 80%. The suppression is particularly strong in the region $z < 1$ nm, where the electroosmotic flow is almost completely quenched. Two physical processes contribute to the observed suppression: (1) the strong electrofriction between the adsorbed counterion and the surface³⁶ and (2) the friction on the fluid and ions rendered by the vertically oriented polymers.^{13,14} The contribution of the electrofriction is important because the electrostatic attraction between the counterion and charged surface atoms is very strong due to the low dielectric constant in the interfacial region.

In summary, we studied the effects of polymer coating on electroosmotic flow near negatively charged surface. For the $(CH_2)_{17}COOH$ polymer studied here, the electroosmotic flow is enhanced slightly at low (11%) grafting density, but is suppressed significantly at high (33%) grafting density. Though the first observation is rarely reported (since typically polymers are coated densely onto the surface), it could occur locally on a nonuniformly coated surface. The latter observation is in line with the earlier experiments in which nonionic polymers coated on the silica

(34) Humphrey, W.; Dalke, A.; Schulten, K. *J. Mol. Graph.* **1996**, *14*, 33.

(35) Varshney, A.; Brooks, F. P.; Wright, W. V. *IEEE Computer Graph. Appl.* **1994**, *14*, 19.

(36) Netz, R. R. *Phys. Rev. Lett.* **2003**, *91*, 138101.

surface can reduce the electroosmotic flow significantly.^{11,12} Although it is difficult to pinpoint the underlying mechanisms from experiments, MD simulations can provide useful insights into these observations. In our simulations, we found that the presence of hydrophobic polymers near the charged surface modify the electrical double layer significantly, and the modulation of electroosmotic flow depends strongly the physical processes inside the electrical double layer. The interfacial polymers affect the electrical double layer by changing the ion hydration and local dielectric constant. At low grafting density, the hydration effects dominate and the ion concentrations near the surface are lowered. The electrical double layer becomes more diffusive, and this leads to a slight increase of electroosmotic flow. At high grafting density, possibly due to a significantly lowered dielectric constant near the surface, a strong adsorption of counterions occurs. In such a case, the electroosmotic flow is suppressed by the electrofriction between the ion and surface and by the drag of polymer on the fluid and ions. We also studied the electroosmotic flow when the surface is grafted with a stiffer polymer (CF₂)₁₇COOH (data not presented here) and found that

flow can be suppressed by 40% at a grafting density of 11%. Together, these results highlight the importance of the electrical double layer and chemical specificity in affecting the electroosmotic flow control. Though this has received little attention from the theoretical community in the past, it can be useful for tailoring the chemical properties of polymer to improve flow control.

It should be noted that, although our detailed MD simulations can capture some fundamental aspects of the electroosmotic flow control, it is computationally very expensive and thus can explore only limited time and length scales. This makes it inefficient for studying the scaling of electroosmotic flow as a function of polymer coating density and external electric field, which has been studied by analytical approaches¹³ and coarse-grained simulations.¹⁵ An ideal method would incorporate the atomistic effects discussed above and at the same time be able to study the flow control at large length scales (e.g., tens to hundreds of nanometers) that is most relevant for engineering practice. Such a method is currently being developed in our laboratory.

LA060883T